ENTATION PAGE

Form Approved
OMB No. 0704-0188

mated to average 1 hour per response, including the time for reviewing instructions, searching existing data sources, gathering and maintaining the data needed, and completing and reviewing the collection of information. Send comments regarding this burden estimate or any other aspect of this s burden, to Washington Headquarters Services, Directorate for information Operations and Reports, 1215 Jefferson e Office of Management and Budget, Paperwork Reduction Project (0704-0188), Washington, DC 20503.

1. AGENCY USE ONLY (Leave blank)	2. REPORT DATE	3. REPORT TYPE AND DATES COVERED
	24 April 1995	Final 1 Feb 93 - 31 Jan 95

4. TITLE AND SUBTITLE
Utilization of Near-Source Video & Ground Motion in the Assessment of Seismic Source Functions from Mining Explosions & Velocity Model & Depth Model, Grefco Perlite Mine

5. FUNDING NUMBERS
PE 61102F
Proj 2309
G AFOSR:
F49620-93-1-0146

6. AUTHOR(S)
David P Anderson, Brian W Stump
Meredith Ness

7. PERFORMING ORGANIZATION NAME(S) AND ADDRESS(ES)
Department of Geology
Southern Methodist University
Dallas TX 75275

8. PERFORMING ORGANIZATION REPORT NUMBER
SMU # 5-25155
AFOSR-TR- 95-0406

9. SPONSORING MONITORING AGENCY NAME(S) AND ADDRESS(ES)
Directorate of Mathematics & Geosciences
Air Force Office of Scientific Research
110 Duncan Ave
Bolling AFB DC 20332-0001

10. SPONSORING MONITORING AGENCY REPORT NUMBER
Seismology Series
95-16

11. SUPPLEMENTARY NOTES
Prepared in cooperation with Los Alamos National Laboratory, EES-3, MS-C335
Los Alamos, NM 87545

12a. DISTRIBUTION/AVAILABILITY STATEMENT
APPROVED FOR PUBLIC RELEASE: DISTRIBUTION IS UNLIMITED

13. ABSTRACT (Maximum 200 words)
Identification of seismic events detected globally at regional distances between the source and the sensor requires a clear physical understanding of the different types of seismic sources including mining explosions, rock bursts, mine collapse, as well as small, shallow earthquakes. This research studies constraint of the operative physical processes in the source region and linkage to the generation of seismic waveforms with emphasis on investigating a number of modern visualization tools that only recently have become available with new, high speed graphical computers that can entertain relatively large data sets. A significant result of this work is the visual manifestation contained in the video tape attached to this report, "Mining Explosions as Seismic Sources". These results provide a basis for identifying the important physical processes at the source that contribute to regionally recorded seismograms. The experiment at the Grefco Perlite Mine was a seismic refraction experiment to determine a consistent velocity and depth model in order to study the source effects. The purpose was to measure the changes in the shock wave and the coupling as a function of depth of burial and structural setting.

14. SUBJECT TERMS
Mining explosions, seismic sources, discrimination, source effects

15. NUMBER OF PAGES
36

16. PRICE CODE

17. SECURITY CLASSIFICATION OF REPORT	18. SECURITY CLASSIFICATION OF THIS PAGE	19. SECURITY CLASSIFICATION OF ABSTRACT	20. LIMITATION OF ABSTRACT
UNCLASSIFIED	UNCLASSIFIED	UNCLASSIFIED	UNLIMITED

UTILIZATION OF NEAR-SOURCE VIDEO AND GROUND MOTION IN THE ASSESSMENT OF SEISMIC SOURCE FUNCTIONS FROM MINING EXPLOSIONS

David P. Anderson
Southern Methodist University
Department of Geological Sciences
Dallas, TX 75275

Brian W. Stump
Southern Methodist University
Los Alamos National Laboratory
EES-3, MS-C335
Los Alamos, NM 87545

AFOSR Grant F49620-93-1-0146

OBJECTIVE: Identification of seismic events detected under a Comprehensive Test Ban Treaty requires a clear physical understanding of the different types of seismic sources including mining explosions, rock bursts, mine collapse and small, shallow earthquakes. Constraint of the operative physical processes in the source region and linkage to the generation of seismic waveforms with particular emphasis on regional seismograms is needed. In order to properly address the multi-dimensional aspect of data sets designed to constrain these sources, we are investigating a number of modern visualization tools that have only recently become available with new, high-speed graphical computers that can utilize relatively large data sets. The results of this study will provide a basis for identifying important physical processes in the source region that contribute to regional seismograms.

RESEARCH ACCOMPLISHMENTS: Mining explosions have been identified as a possible source of seismic signals that at small magnitude might have to be discriminated from a nuclear explosion, possibly tested in a clandestine environment. Many mining explosions occur each year as documented by Richards *et al.*, 1992. The coupling as well as the source characterization of these events must be investigated in order to assess the possible impact they might have on a monitoring system. The source characterization studies are directly linked to attempts to discriminate events based upon the relative excitation of different regional phases and the spectral content of the signals. One of the most discussed discriminants has been spectral scalloping of the signals resulting from either the delay times between the individual charges in the mining explosion or the total duration of the shot. The literature contains many studies that attribute this possible discriminant to one of these mechanisms with no consensus on the cause (Baumgardt and Ziegler, 1988; Hedlin *et al.*, 1989; Hedlin *et al.*, 1990; Smith, 1989; Chapman *et al.*, 1992). None of these studies made any direct observations of the blasts that could confirm or deny the

conclusions of the analysis of the regional data. In some cases, official blasting records from the mines were available for comparison but as Stump *et al.*, 1994 point out these records sometimes are in disagreement with actual blasting practices. In addition to spectral differences, a number of authors have investigated the generation of regional P, S and surface waves by mining explosions and have suggested the use of the relative excitation of these phases. Modeling to accompany these studies has attempted to quantify the relative importance of the directly coupled energy from the explosions, vertical and horizontal spall, the rubblization process and the three dimensional structure of the mine itself on the resulting regional waveforms (Barker and McLaughlin, 1992; McLaughlin *et al.*, 1993).

Following the work of Reamer *et al.*, 1992 this paper reports on efforts to document physical processes in the near-source region of mining explosions for the purposes of unambiguously constraining the important characteristics of mining explosions that generate seismic waves. Studies such as this in conjunction with regional observations from the same events provide the mechanism for placing regional discriminants on a firm physical foundation that can then be extrapolated to new environments or locations. The recent Non-Proliferation Experiment (Denny and Zucca, 1994) illustrates one such controlled experiment in which a combination of near-source and regional measurements were used to explore the similarities and differences of chemical and nuclear explosions.

Mining explosions are designed for a variety of purposes including the fragmentation and movement of materials. The blast design is dependent on the particular application intended and the material properties of the rock. The range of mining applications from hard rock quarrying to coal exposure to mineral recovery leads to a great variety of blasting practices. A common component of many of the sources is that they are detonated at or near the earth's surface and thus can be recorded by camera or video. Although our primary interest is in the seismic waveforms these blasts generate, the visual observations of the blasts provide important constraints that can be applied to the physical interpretation of the seismic source function. In particular, high speed images can provide information on detonation times of individual charges, the timing and amount of mass movement during the blasting processes and in some instances evidence of wave propagation away from the source. All of these characteristics can be valuable in interpreting the equivalent seismic source function for a set of mine explosions and quantifying the relative importance of the different processes. This report documents an attempt to take standard Hi-8 video of mine blasts, recover digital images from them and combine them with ground motion records for interpretation. The steps in the data acquisition, processing, display and interpretation will be outlined. Two applications, the first a single cylindrical charge at standard burden distances and a small, four-by-four, ripple-fired explosion will be used to illustrate the techniques.

The blasts were all recorded on a Sony TR101 Hi-8 video camera at 30 frames/s and a 1/10000 shutter speed. The camera was deployed approximately 100 m from the single cylindrical charge parallel with the free face in front of the charge. During the ripple-fired explosion, the camera was deployed approximately 250 m behind and above the explosion. In each deployment, there was a near-by ground motion sensor for correlation with the video. The ground motion data was acquired with a 16-bit

Refraction Technology Data Acquisition System. Terra Technology accelerometers and Sprengnether S-6000 2 Hz seismometers. The focus of this discussion will be on the video acquisition and processing as the ground motion data was processed in standard ways.

The raw video images were transferred to a Sony CVR 5000 laser disk using the Silicon Graphics Inc. (SGI) Galileo Card for time-base correction, a process which takes a few seconds. 150 frames (i.e., 30 fps * 5 sec) of the video were digitized outside of real-time from the laser disk and transferred to hard disk using the SGI Galileo Video card. This process produces YUV format color images each 640x486 pixels for a total size of 150 MBytes. The files are converted from YUV to RGB format and written as Run Length Encoded (RLE) files using the Utah Raster Toolkit conversion utility (URT tools are available free from the ftp anonymous login cs.utah.edu). At this point each individual frame of the image consist of two interlaced fields sampled 1/60 sec apart. Figure 1 illustrates one of the interlaced frames from the single, cylindrical explosion. The fuzzy nature of the image is due to the rapid speed at which the material is moving and the interlacing of two fields sampled 1/60 sec apart to produce a single video frame.

Figure 1: Raw, interlaced video frame from the single cylindrical explosion. The frame follows the detonation of the explosive by 500 msec.

The frames are next de-interlaced and interpolated into one even and one odd field which represent two instances in time separated by 0.01667 sec. Additional contrast and image enhancement is performed on the de-interlaced images using RLE public domain utilities. The marked improvement in the image quality after these steps is illustrated in Figure 2

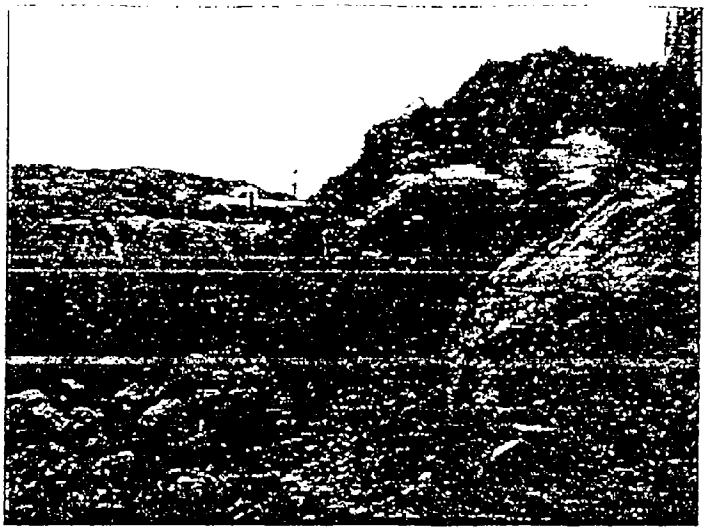

Figure 2: De-interlaced and image enhancement of the even field from the frame displayed in Figure 1.

Although not obvious in the single frames and fields displayed in this paper, the camera moves as the P wave arrives at the recording site. This motion degrades the interpretation of the blast and so a simple correction scheme called de-jittering was devised. The location of a stationary distant point or points is noted in each frame and then the field is corrected to this location to remove camera motion. The resulting corrections for all the frames in the video are combined to produce a representation of the camera motion in the plane of the picture. The individual frames are then combined and animated on the SGI to produce a digital record of the blast at 0.01667 sec resolution. *An animated representation of these images will be available for review at the meeting.*

The final step of the process is to combine the digital video images with the digital ground motions so that one can begin to investigate the relationships between the ground motion and the source processes as recorded by the camera. The ground motions are superimposed on the bottom of the video frame along with a vertical cursor that indicates the location in time of the waveform relative to the image currently being viewed. Time correlation between the video images and the ground motion records is made with the P arrival record. The composite animation are next reconverted to RGB format and sequenced one frame at a time back onto the laser disk. The laser disk can then be used to play the animation at speeds from 30 frames per second (1/2 real time after de-interlacing) to a single frame stop motion. We have found that the ability to interact with the animation at various speeds has been one of most important visualization tools. An example of one frame from the composite is given in Figure 3.

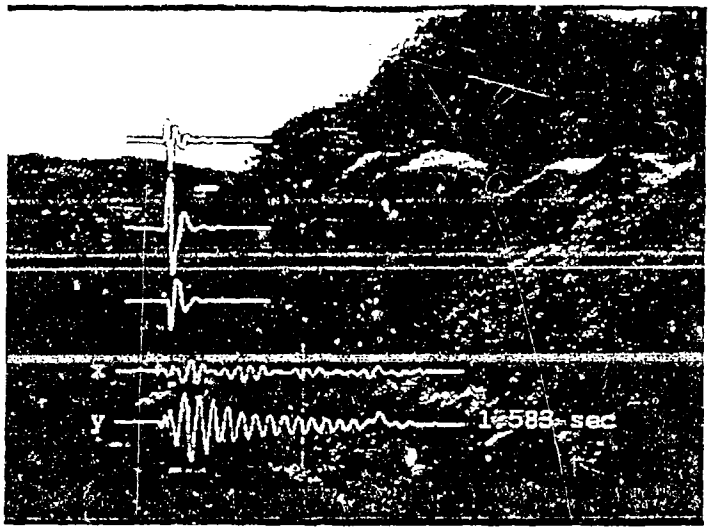

Figure 3. De-interlaced, de-jittered and composited field from the single, cylindrical explosion. The bottom two time series are the recovered camera displacements from the de-jittering process (x-tangential, y-vertical). The top three time series are ground velocities (vertical, top; radial, second; transverse, bottom) derived from a near-by accelerometer. Time denoted in the figure is elapsed time since the detonation of the surface delay.

The vertical bar in Figure 3 denotes the time in the waveforms that correlate with the video field from the explosion. Comparison of the ground motion record with the camera displacements illustrates the under damped pendulum response of the camera tri-pod. The near-source ground motions are completed many msec prior to this video image. The image also illustrates that there are still many dynamic processes taking place in the source region despite the lack of ground motion. Careful review of the animation reveals the importance of the initial shock from the explosive in generating the near-source ground motions. The P wave as it propagates from the initial shock to the camera can be seen as a reflectance change in the near-surface materials. These two observations indicate that for the recorded near-source ground motions that late time explosion phenomena including the material that is cast out into the pit do not contribute to these waveforms.

The same processing scheme was applied to the ripple-fired explosion. In this case, one can identify the non-electric detonating system as it operates, the detonation of the individual charges, the interaction of the motion between the individual charges and the spall of the material. The frame rate of the video is not fast enough to constrain the exact detonation time of all the surface delays. High speed film or video with frame rates as high as 500 frames/s are more appropriate for this task. Figure 4 illustrates one field from the ripple-fired explosion.

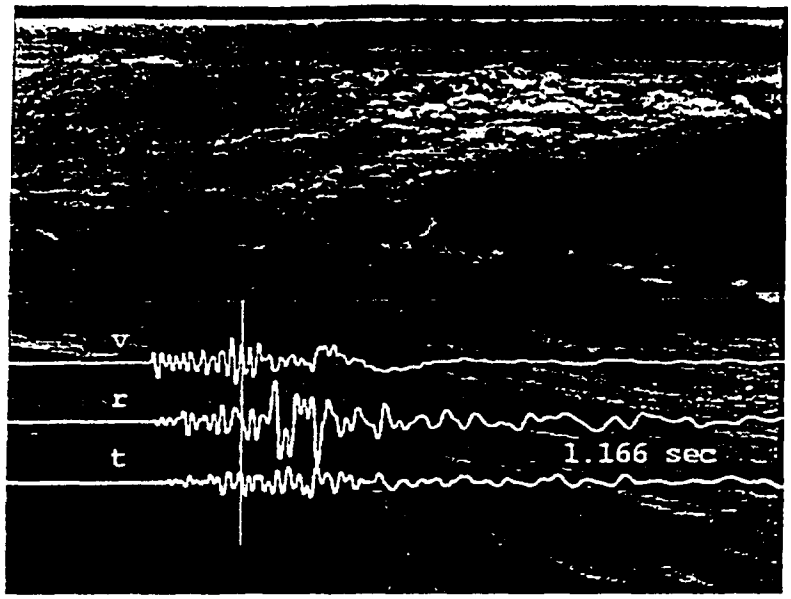

Figure 4: De-interlaced, de-jittered and composited filed from the ripple-fired explosion. The ground velocities and the camera are at a range of approximately 250 m from the explosion.

CONCLUSIONS AND RECOMMENDATIONS: The utility of combining video records and ground motion records from the near-source region of mining explosions has been demonstrated. This tool provides a unique opportunity for investigating the physical properties important in generating seismic waveforms. The simple examples presented in this paper argue that direct shock coupling of energy from the explosion is of primary importance in the generation of near-source waveforms and that the material cast by such explosions is of secondary importance. Analysis of the ripple-fired explosion documents the firing sequence and the cylindrical interaction of the individual charges in the source array. Spall processes quantified by the video occur at late time relative to the near-source motions.

Simple Hi-8 video with its improved resolution provides the starting point for this analysis procedure. The key to the work is the digitization of the video, the de-interlacing, the de-jittering and the animation with the recorded waveforms. A modest priced desk top computer such as a SGI Indigo-2 coupled with a video capture card provides the basis of the analysis system. A read/write laser disk system is needed as well for both the processing steps and the final assembly of the images.

This preliminary study has begun to explore the utilization of different types of data in the interpretation of the seismic source function. Additional work with multiple cameras intended to provide three-dimensional characterization of the source is planned. These images can be used to provide detailed temporal and spatial quantification of material motion in the source region. These same images in combination with sparsely sampled ground motion records can be used to provide some understanding of the two and three dimensional aspects of the seismic wavefield. We intend to explore the utilization of the video images as an interpolating tool between the point ground motion records.

An important key to these visualizations is the linking of temporal and spatial aspects of the problem in a logical way so that the scientists can interpret the important physical processes in the source. *Processed video records of the tests discussed in this paper will be displayed at the meeting for those interested in investigating the temporal and spatial relations in the video and ground motion data sets.*

REFERENCES

Baumgardt, D. R. and K. A. Ziegler, Spectral evidence for source multiplicity in explosions: Application to regional discrimination of earthquakes and explosions, *Bull. Seismol. Soc. Am., 78*, 1773-1795, 1988.

Chapman, M. C., G. A. Bollinger and M. S. Sobel, Modeling delay-fired explosion spectra at regional distances, *Bull. Seismol. Soc. Am., 82*, 2430-2447, 1992.

Denny, M. D. and J. J. Zucca, Introduction: DOE Non-Proliferation Experiment, *Arms Control and Nonproliferation Technologies, First Quarter 1994*, 8-21.

Hedlin, M. A. H., J. A. Orcutt, J. B. Minster, and H. Gurrola, The time-frequency characteristics of quarry blasts and calibration explosions recorded in Kazakhstan, U.S.S.R., *Geophys. J., 99*, 109-121, 1989.

Hedlin, M. A. H., J. B. Minster and J. A. Orcutt, An automatic means to discriminate between earthquakes and quarry blasts, *Bull. Seismol. Soc. Am., 80*, 2143-2160, 1990.

Reamer, S. K., K.-G. Hinzen and B. W. Stump, Near-source characterization of the seismic wavefield radiated from quarry blasts, *Geophys. J. Int., 110*, 435-450, 1992.

Richards, P. G., D. A. Anderson and D. W. Simpson, A survey of blasting activities in the United States, *Bull. Seismol. Soc. Am., 82*, 1416, 1992.

Smith, A. T., High-frequency seismic observations and models of chemical explosions: Implications for the discrimination of ripple-fired mining blasts, *Bull. Seismol. Soc. Am., 79*, 1089-1110, 1989.

Stump, B. W., F. Rivière-Barbier, I. Chernoby and K. Koch, Monitoring a Test Ban Treaty Presents Scientific Challenges, *EOS, Trans. Am Geophys. U., 75*, 265-273, 1994.

ACKNOWLEDGMENTS. Some support for BWS was made possible by the Department of Energy and the Source Region Program at Los Alamos National Laboratory. John Smith, John Wiggins and R. Frank Chiappetta are thanked for their support in the field. D. Craig Pearson, Meredith Ness and Ben Smith were responsible for the data acquisition.

VELOCITY MODEL AND DEPTH MODEL OF THE GREFCO PERLITE MINE

Meredith Ness

ABSTRACT

A series of small-scale explosive ground motion experiments were conducted by Los Alamos National Laboratories and Southern Methodist University in the Grefco Perlite Mine near Socorro, New Mexico. The purpose of the experiments was to measure the changes in the shock wave and seismic coupling as a function of depth of burial and structural setting. In order to understand the structural effects on the seismic waveforms, Southern Methodist University conducted a refraction experiment at the mine. The purpose of the refraction experiment was to determine a consistent velocity model and depth model for the site. With a consistent structural model of the site and explosive waveforms, the source effects can be studied. The interpretation of the refraction data yielded a consistent velocity model with approximate velocities of 266 meters/second, 645 m/s, and 1210 m/s. The upper layer consists generally of loose material and was determined to be a weathered layer. The Poisson's ratios for the first and second layers were calculated to be 0.24 and 0.16 respectively.

CONTENTS

LIST OF FIGURES

INTRODUCTION

Detection, discrimination, and characterization of underground explosions are important in the move towards the nonproliferation of nuclear weapons. As part of an effort to understand explosion waveforms in different media, Los Alamos National Laboratories (LANL) conducted a series of experiments to study the explosion waveforms in perlite. Southern Methodist University (SMU) participated in recording the ground motion from the explosions and conducted refraction experiments to determine a consistent velocity model and depth model for the site. This report presents the velocity model and depth model calculated from the SMU refraction data and two previous experiments.

A preliminary refraction study was conducted by Allen Cogbill of LANL. His data is reinterpreted and included as part of the data set. Also included in the data set is the refraction data from three small-scale high explosive shots collected by the Geophysics Group, EES-3, LANL in conjunction with SMU (Edwards, Pearson and Baker 1994).

This report is unique for several reasons. First, several different sources including high stress and low stress sources were used to generate P wave and shear wave-data. Both the preliminary refraction study and the SMU refraction study used low stress sources. The three small-scale high explosive shots were high stress sources that were buried at depth. Second, the data set has a high resolution due to the number of data points used. Third, two different interactive computer programs were used to interpret the data. REFRACT was written by Craig Pearson of LANL using MATLAB software. REFRACT is a simple program based on a one-dimensional plane layered interpretation of the data. The second program is a commercial software package called SIP (Seismic Interpretation Program). SIP is a more complicated program that creates a 2 ½-dimensional cross-sectional depth model.

SITE DESCRIPTION

The experiment site is in the Grefco Perlite Mine located near Socorro, New Mexico. The experiments were conducted in an area that has been previously mined and is oblong in shape (Figure 1). There are two major fracture sets present on the experiment floor (Edwards, Pearson and Baker 1994). The axis of the major fracture set strikes at approximately 0° and runs parallel to the refraction line, and the axis of the second fracture set strikes at approximately 300°. The mine floor sloped gently downwards to the north and consisted of various sizes of perlite fragments and *in situ* perlite.

Figure 1: Photograph of Experiment Site

MATERIALS AND METHODS

Originally the SMU refraction experiment was designed with two refraction lines oriented perpendicular to each other. The first refraction line was oriented north-south and corresponds with the main instrument line from the previous small-scale explosion experiments conducted by LANL and SMU (Figure 2). No experiments were conducted along the second refraction line due to time constraints.

Figure 2: Aerial Photograph of Experiment Site

Two sources were used to generate energy. A Betsy Seisgun was used for the P wave source (Figure 3). A Shear Wave Impulse Generator (SWIG) was used to generate shear waves. The SWIG is a pneumatic hammer that can be shot in two directions to reverse the polarity (Figure 4).

Figure 3: Betsy Seisgun - P Wave Source

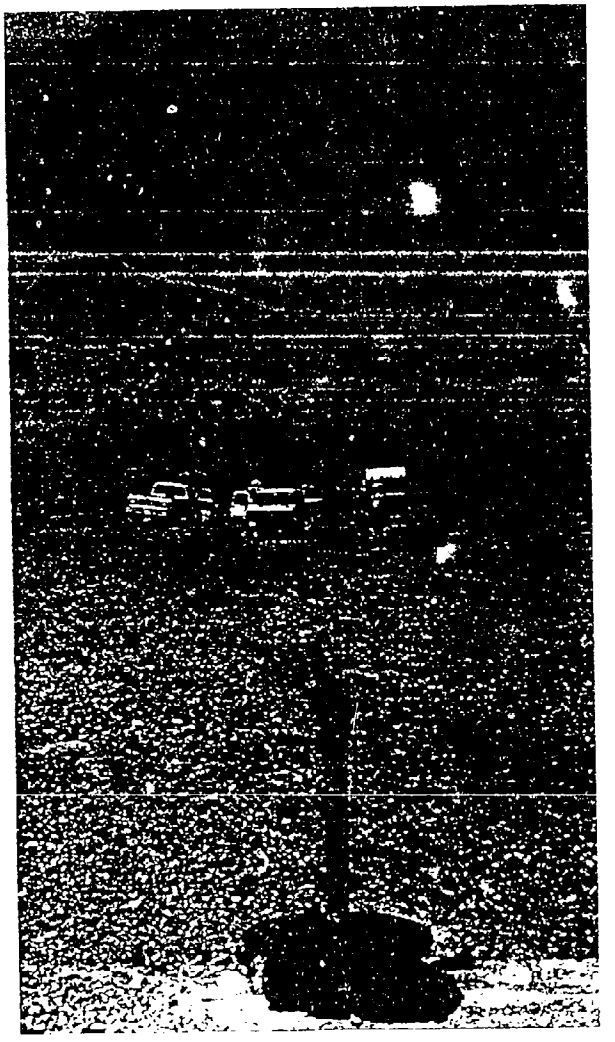

Figure 4: SWIG - Shear Wave Source

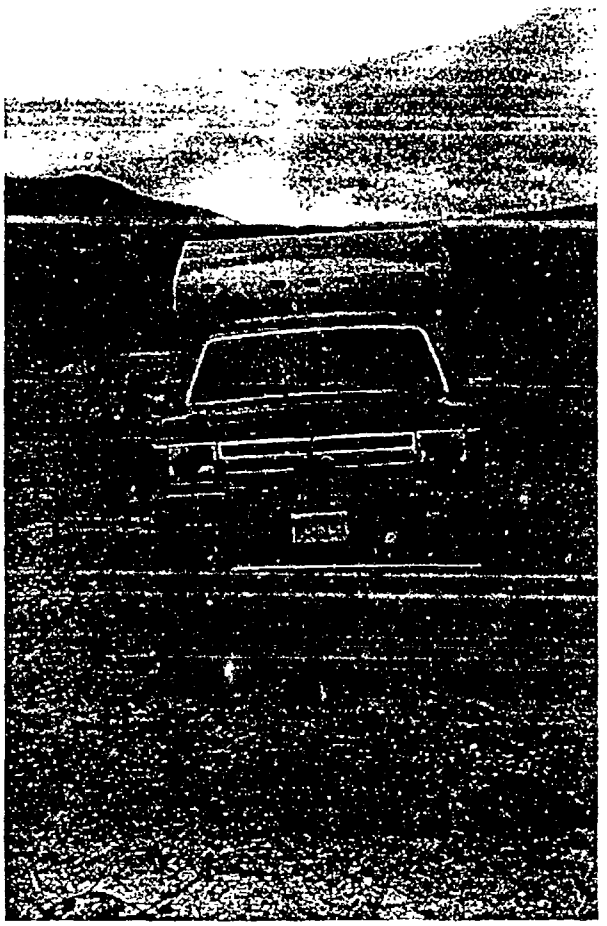

Vertical geophones (10 Hz) were used for collection of the P wave data, and horizontal geophones (10 Hz) were used to collect the shear wave data. The horizontal geophones were oriented to the east at right angles to the refraction line. The data was recorded by an EG&G twelve-channel recorder (Figure 5). For the second set of experiments, an array of twelve geophones was connected to the EG&G recorder. After obtaining good data recordings, the geophones were disconnected and the next array of twelve geophones was connected. Then recordings were made from the same shotpoint.

Figure 5: EG&G Twelve-Channel Recorder

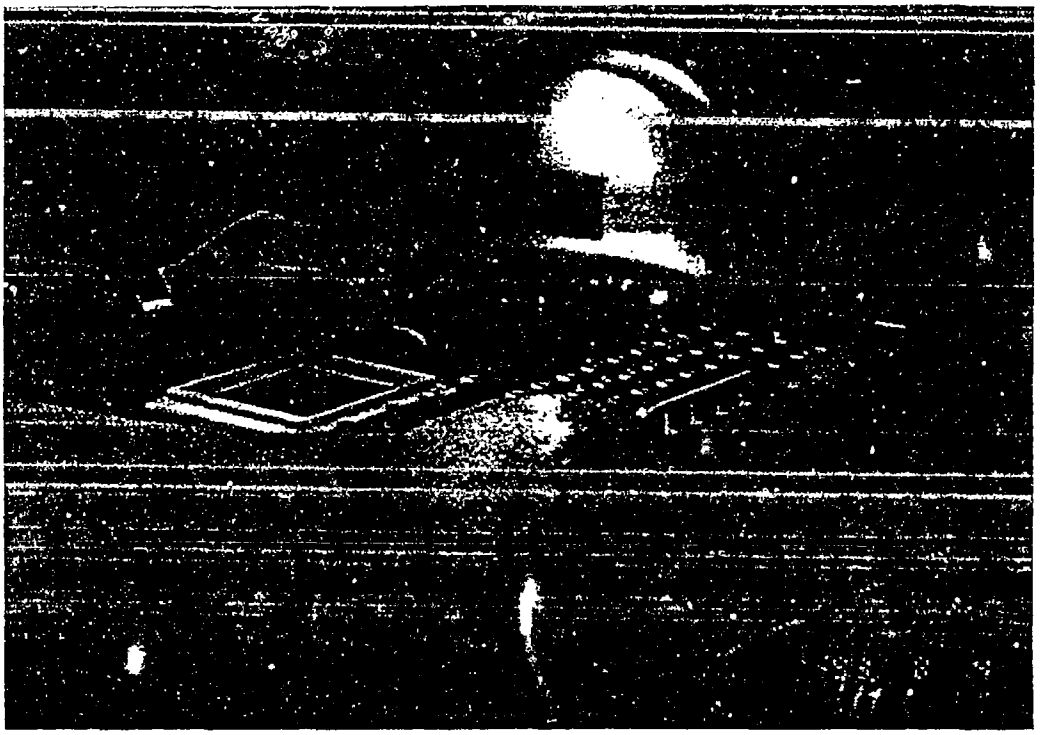

The first set of refraction work was done on August 2, 1993. The refraction line consisted of twelve geophones labeled A2 (array 2) and eight shotpoints (Figure 6). The geophones were spaced at 2 meter intervals with the first geophone 56 meters from the 150-lb. LANL shot hole. Four shotpoints were placed both north and south of the array. Shotpoint 1 (S1) and shotpoint 5 (S5) are 2 meters from the nearest geophones. All other shotpoints were placed 20 meters from the previous shotpoint except for shotpoint 8 (S8) which is only 18 meters from shotpoint 7 (S7). P wave experiments were conducted at all eight shotpoints, while shear wave experiments were conducted at S1, S2, S5 and S6.

Figure 6: SMU Experiment Layout from 8/2/93

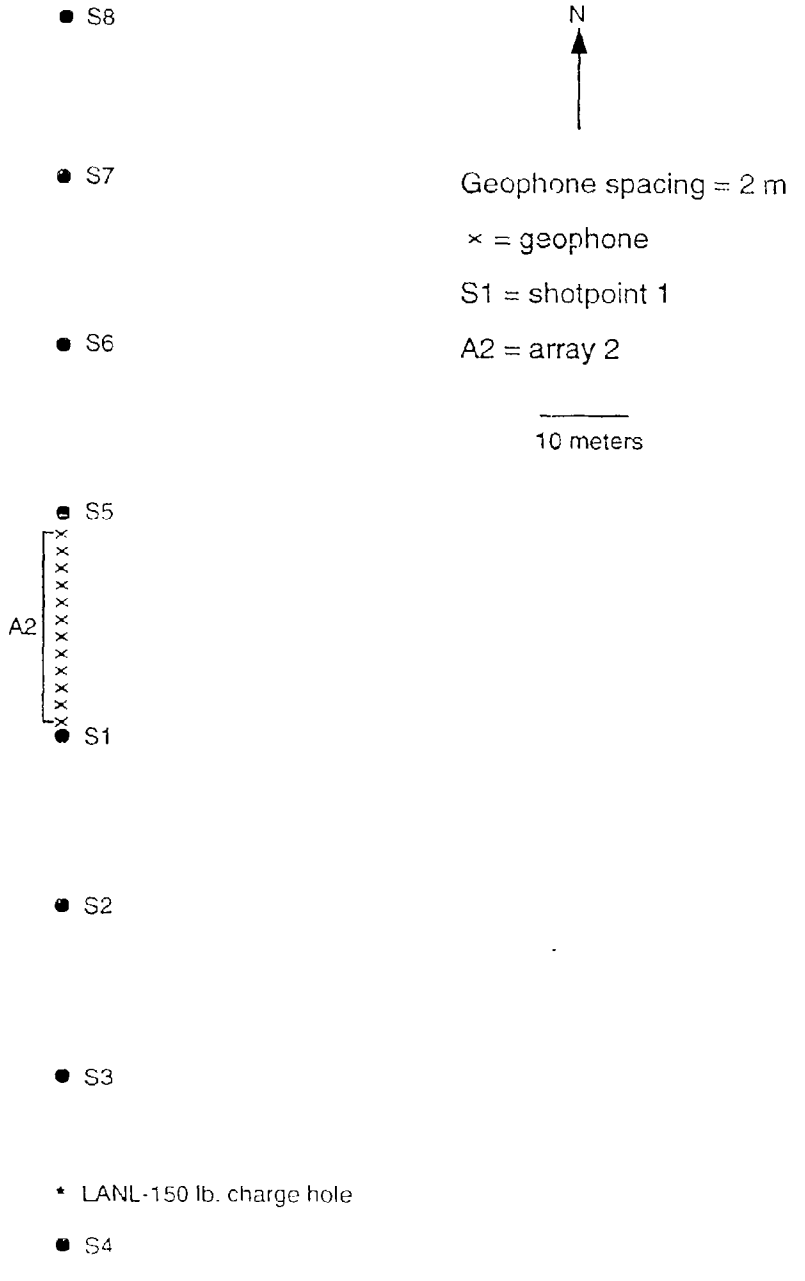

Due to the preliminary analysis of the P wave and shear wave data on August 3, further refraction work was conducted on the 4 and 5 of August. A 36 element array with four shotpoints was installed (Figure 7). Again, the geophones were spaced at 2 meter intervals. The first geophone is located 32 meters from the 150-lb. LANL shot hole. Two shotpoints were placed 2 meters from the nearest geophone at the ends of the array, and two more shotpoints were placed in the middle of the array just offset from the geophones. The twelve center geophones, labeled A2 (array 2), correspond to the array from August 2. Geophone locations were pre drilled (Figure 8) to improve receiver coupling by wedging the geophone spikes into the holes (Figure 9). Sandbags were placed on top of the geophones to reduce the amount of wind generated background noise.

The arrival time data were analyzed using two different interactive interpretation programs. Craig Pearson wrote REFRACT using MATLAB software. REFRACT assumes that the layers are planar and that velocities remain constant throughout the layers. An M file was created for both the P wave and shear wave data. Each M file contains the range and arrival times for each shot. REFRACT calls the M file and plots the data as range versus time for a particular shotpoint and corresponding array(s). After the data is plotted, one determines the number of layers and selects the crossover points between the layers. After each crossover point is identified, a line is automatically fit to the appropriate data segment. When all the layers have been identified, REFRACT calculates the velocity and thickness for each layer using both intercept times and crossover distances. This information is tabulated on each plot of arrival time data.

Figure 7: SMU Experiment Layout from 8/4/93 - 8/5/93

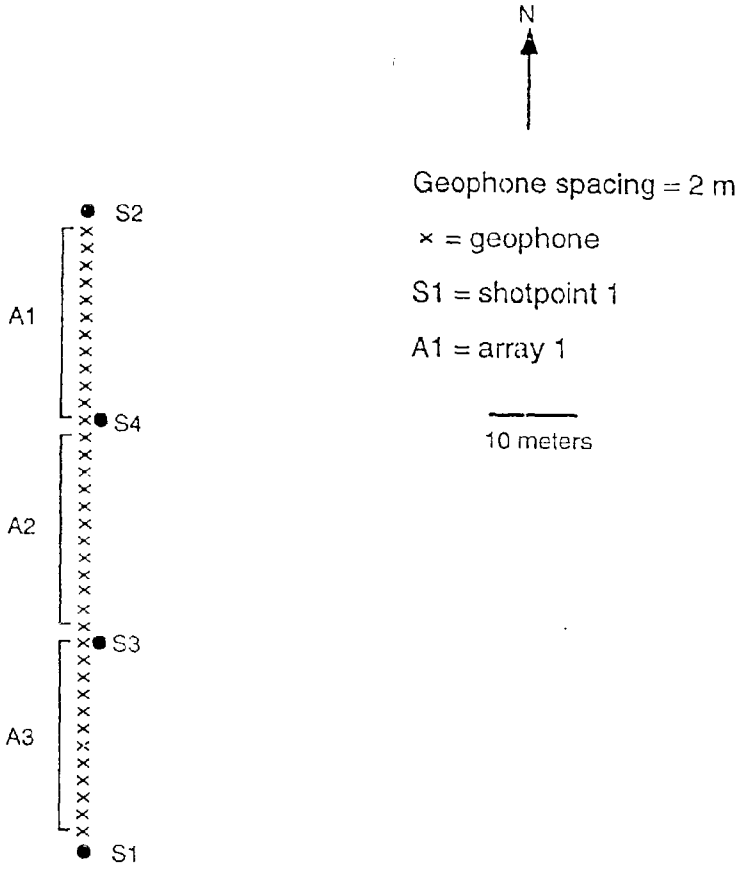

* LANL 150 lb. charge hole

Figure 8: Drilling Geophone Holes

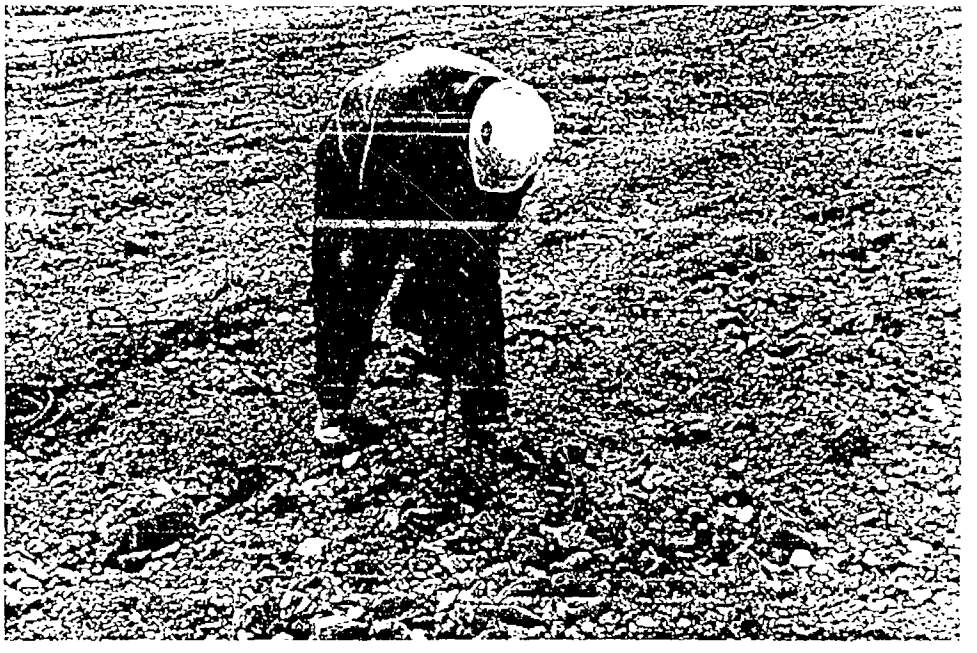

Figure 9: Emplacement of a Geophone Into a Pre Drilled Hole

SIP is a DOS shell program used for running seismic refraction programs created by Rimrock Geophysics (SIP reference). Three of the available programs were used: SIPIN, SIPEDT, and SIPT2. SIPIN creates input data files for use in other SIP programs (SIPIN reference). Up to five spreads can be entered for each data set. After the spread geometry is specified, the arrival times and elevations for each geophone are entered by hand. The elevations were calculated from the surveyed elevations of the main instrument line from the earlier LANL/SMU experiment. Next, the data was plotted as a time-distance plot. Then each arrival time is assigned a 1, 2, or 3 to designate in which layer the ray bottomed. SIPT2 also allows internally computed velocities to be overridden. Velocity override values can be entered in SIPIN or SIPEDT forcing SIPT2 to replace the internally computed velocities with the override velocities. Once all the data has been entered, the data file is written to disk.

SIPEDT is used for editing existing data and entering new data into the data files (SIPEDT reference). The data file to be edited is selected. From the SIPEDT main menu, one can choose the part of the data file that requires modification. SIPEDT is particularly useful because it makes the data file easy to edit without having to create a whole new data file with SIPIN.

SIPT2 is the program that interprets the refraction data (SIPT2 reference). The velocity for each layer is computed by regression and the Hobson-Overton method (a least squares version of the reciprocal time difference method) if there are enough reciprocal points. Then the geophones and shotpoints are shifted to a sloping datum plane fitted through the geophone positions. A first-approximation depth model is made by SIPT2. The depth model is obtained by an inversion algorithm that is based on the delay-time method (Pakiser and Black 1957). The model is then refined by a series of ray-tracing and model adjustment iterations. The measured arrival times and computed arrival times traced through the depth model are compared and adjusted to

minimize the discrepancy between travel times. The other layers are computed in the same manner after the overlying layer has been mathematically stripped away. A final iteration is made through all the layers to correct for near surface anomalies.

INTERPRETATION

P Wave Data

A total of 44 P wave record sections were recorded (Appendix G). The background noise level for all three days varied depending upon the wind and machinery running at the mine. First-arrivals were picked by hand from the traces with the best signal to noise ratio. Estimated errors in arrival times are 3 milliseconds. From the first refraction experiment, arrival times were picked for shotpoints 1, 2, 3, and 4 out to approximately 60 meters. Arrival times were picked out to approximately 40 meters for shotpoints 5, 6, 7, and 8.

The data from the second experiment was generally better than the data from the first experiment. The signal to noise ratio was higher for the second experiment. Furthermore, the shotpoints were stationary while the array moved. This negated the moveout effect from the first experiment. From the second refraction experiment, first arrivals were picked out to approximately 50 meters for shotpoint 1 arrays 3, 2, and 1. The data from shotpoint 2 arrays 1, 2, and 3 (S2A123) was much better and first arrivals were picked for all traces (72 meters).

Shots from two points within the arrays (S3 and S4) were anticipated to help constrain the velocity and depth models; however, their analysis did not prove to be particularly useful. The data from shotpoint 3 array 3 (S3A3) yielded a first layer velocity approximately 100 meters/second slower than the data from S1A321 and S2A123. The second layer velocity calculated from S3A3 data was about 200 m/s

faster than the velociy calculated using the data from S1A321 and S2A123. The data from shotpoint 4 array 3 (S4A3) yielded a third layer velocity approximately 200 m/s slower than the velocity calculated from S1A321 and S2A123.

Since the data from the second experiment tends to be better, the P wave model is based on the interpretations of S1A321 and S2A123. Both types of interpretations returned similar results for the data from the second experiment. The data from S1A321 (shotpoint 1 - arrays A3, A2, and A1) and S2A123 (shotpoint 2 - arrays A1, A2, and A3) interpreted by REFRACT yielded the following approximate velocities:

layer one = 280 meters/second

layer two = 665 m/s

layer three = 1230 m/s.

The depth to the first refractor is about 1.5 meters, and the depth to the second refractor is about 6.5 meters. The results for the data interpreted by REFRACT are in Appendix D.

One of the advantages of SIPT2 is that the reverse spreads (S1A321 and S2A123) could be interpreted at the same time, thus producing a more consistent model. The files labeled as Combo1s and Combo in the SIP output files, produced the following velocities:

layer one = 251 m/s

layer two = 625 m/s

layer three = 1190 m/s.

Combo1s and Combo both use the data from the reverse spreads S1A321 and S2A123. The difference between the two files is that Combo1s combines all the arrays into one spread with two shotpoints (S1 and S2) and Combo uses two spreads with one shotpoint each. Combo1s allows SIPT2 to create a depth model using

reciprocal arrivals to compute velocities. With Combo, SIPT2 computes a separate depth model for each of the two spreads and superimposes them in the depth plot. The difference between the two depth models is minimal. The depth model computed using Combo1s is shown in Figure 10. Since SIPT2 can interpret undulating surfaces, the depths to the refractors are listed in the output files in Appendix F.

Based on the models, the first layer is interpreted as the weathered layer. The weathered layer approximately follows the topography except for where it pinches out at approximately 14 meters from S1 (see Figure 10). The most competent perlite was extracted from that part of the test bed indicating that this material has not weathered as much as the surrounding material. The second layer could be due to a change in the depositional flow banding or an overburden effect.

Shear Wave Data

A total of 47 shear wave record sections were recorded (Appendix L). The shear wave data was considerably harder to interpret because the signal to noise ratio was reduced and first arrivals were more difficult to identify. First arrivals were picked four times to obtain the best possible arrival times. In order to help identify first arrivals, a record section was collected from the SWIG source fired in each of its two directions perpendicular to the refraction line. The shear arrivals for these two source orientations were 180° out of phase. Superposition of the two record sections provided the means for shear wave identification based on the 180° phase change. The last picks were used for the shear wave interpretations.

The best shear wave traces are from the first experiment (see Figure 6) which had a higher signal to noise ratio. The SWIG was shot at shotpoints 1, 2, 5, and 6. Shotpoints 1 and 2 are combined in a file labeled S12, and shotpoints 5 and 6 are combined in a file labeled S56. For these shotpoints, I picked arrival times out to approximately 40 meters. The data set from the second experiment contains arrival

Figure 10: SIPT2 Depth Model for Combo 15

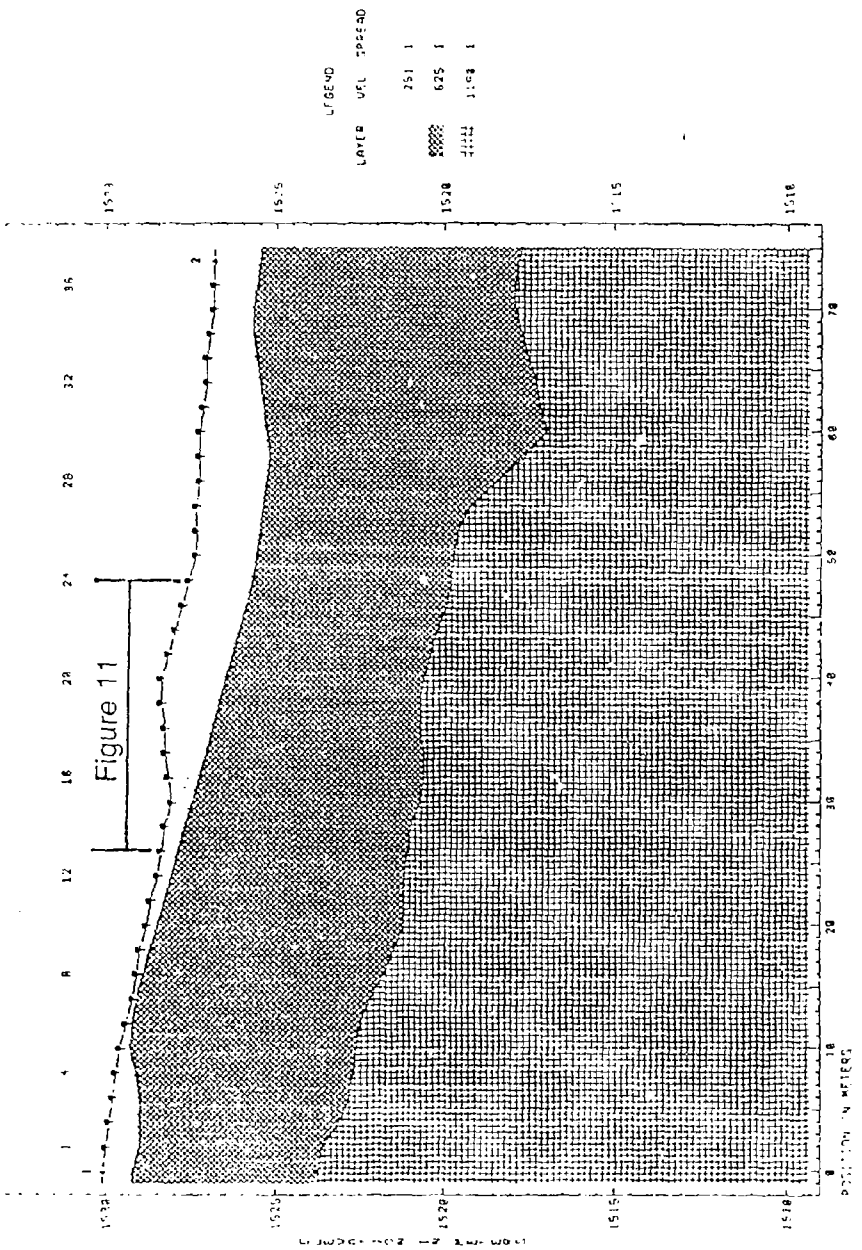

times out to about 36 meters. The estimated error in arrival time is 5 ms. Neither polarity direction (east or west) consistently produced superior waveforms. This is probably due to the highly fractured nature of the rock and anisotropy.

A hammer was used during the second refraction experiment (see Figure 7) as a source for one of the records from shotpoint 2 array 1. The record section and corresponding files are labeled S2A1 - Hammer. The data obtained from the hammer was not very good. The shear velocities for the first and second layer were consistently 200 m/s higher than the other calculated shear velocities.

Again, both programs returned similar results. Since the shear data from the first experiment is better, the shear wave model is based on the interpretation of S12 and S56. REFRACT computed the following average velocities:

layer one = 150 meters/second

layer two = 416 m/s.

The depth to the first refractor is between 1 meter and 1.8 meters. The results for the data interpreted by REFRACT are in Appendix J.

Using SIPT2, S12 and S56 were combined into two files labeled S1256 and S161s. S1256 interprets array A2 with shotpoints 1 and 2 seperate from array A2 with shotpoints 5 and 6. S161s interprets array A2 with shotpoints 1, 2, 5 and 6 simultaneously. The following velocities were computed for both S1256 and S161s:

layer one = 155 meters/second

layer two = 408 m/s.

Like the P wave SIPT2 interpretations, the difference in the depth models of S1256 and S161s is minimal. The depth model computed using S1256 is shown in Figure 11, and the output files are in Appendix K.

P Wave and Shear Wave Results

Both the P wave and shear wave interpretations are consistent with each other. The depth to the first refractor computed by REFRACT from both P waves and shear waves is similar. In the SIPT2 depth model plot for SHCOMBO spread 1 (Figure 12), the same rise in the first refractor at about 14 meters from S1, which is 2 meters to the left of the geophone labeled 1, is observed although it is less pronounced than in the P wave model. The shear data also supports the conclusion that the first layer is a weathered layer since the refracting surface generally follows the surface. The Poisson's ratios for the first and second layers were calculated to be 0.24 and 0.16 respectively.

Cogbill Data

The preliminary refraction data collected by Allen Cogbill of LANL was reinterpreted and checked for consistency with data from this study. Cogbill collected and interpreted the data before the small-scale high explosive LANL/SMU experiments were conducted, and interpreted the data as a continuos increase in velocity (Edwards, Pearson and Baker 1994). The geophones were spaced at two meter intervals, and the refraction line was oriented north-south were the main instrument line for the LANL/SMU experiments would later be placed. Figure 13 compares the SMU refraction layout, Cogbill's refraction layout and the LANL/SMU main instrument line.

Cogbill's refraction data is interpreted here in the same manner as the SMU P wave data. REFRACT computed the following average velocities:

layer one = 540 meters/second

layer two = 800 m/s

layer three = 1306 m/s.

Figure 11: SIPT2 Depth Model for S1256

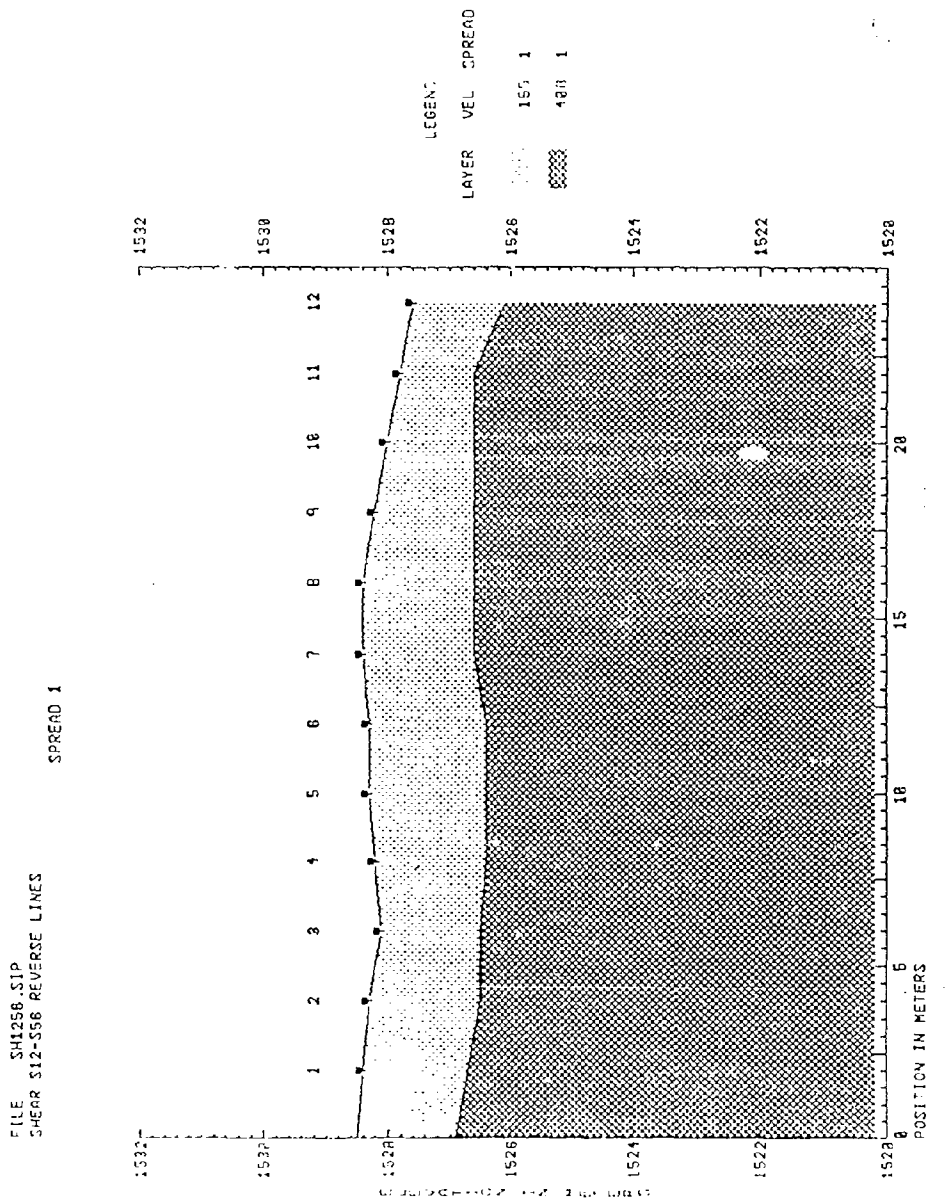

Figure 12: SIPT2 Depth Model for Shcombo, Spread 1

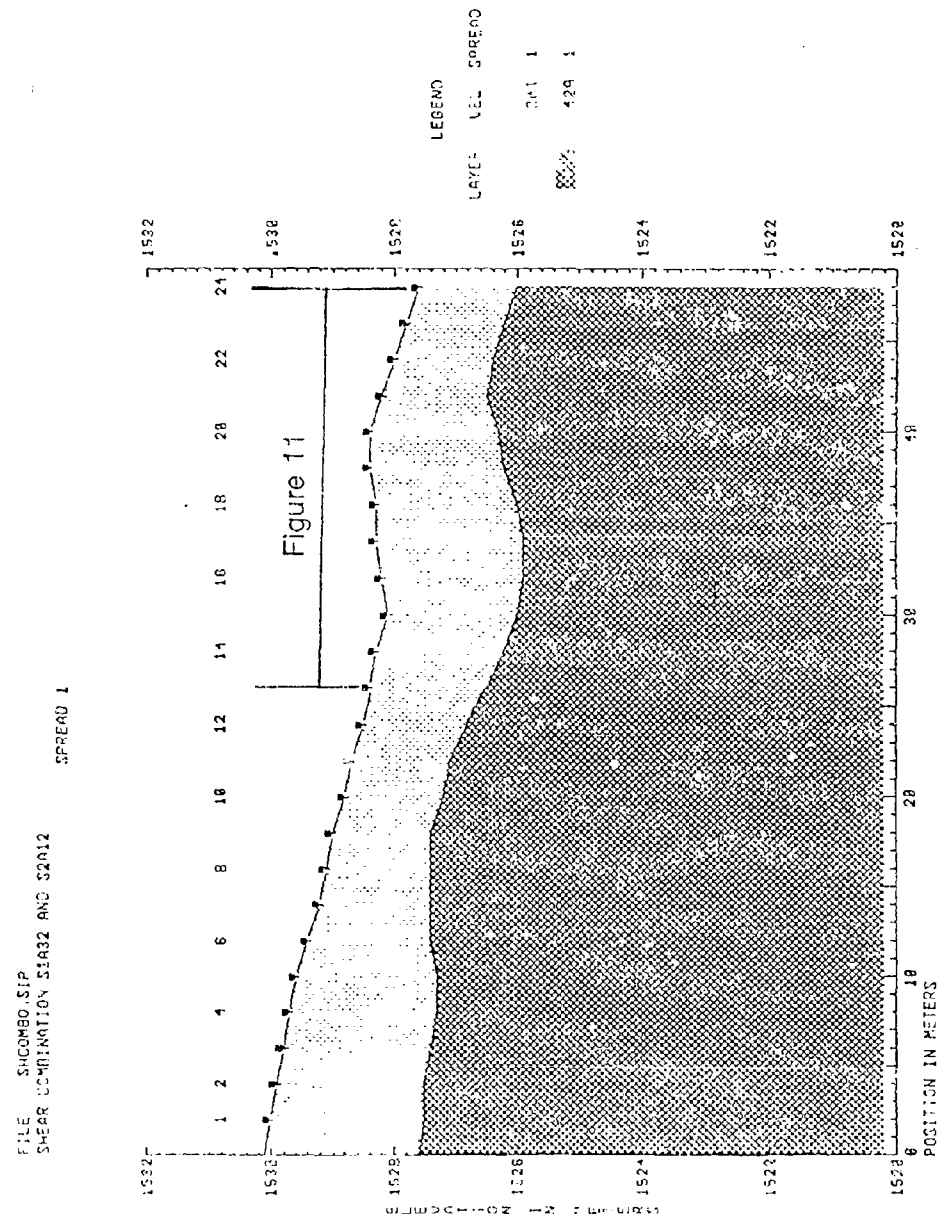

Figure 13: Comparison of SMU Refraction Layout, Cogbill Refraction Layout and LANL/SMU Main Instrument Line

The depth to the first refracting horizon is between 2.5 meters and 4 meters. The results computed by REFRACT are in Appendix O.

Using Cog13c, which is a combination of data files Cog1 and Cog3, the following velocities were computed:

layer one = 158 meters/second

layer two = 738 m/s

layer three = 1440 m/s.

The depth model for Cog13c is shown in Figure 14. The output files for SIPT2 are in Appendix P.

Both sets of velocities computed from Allen Cogbill's refraction data are approximately 200 m/s faster than the P wave velocities computed from SMU's P wave data. Perhaps Cogbill's signal to noise ratio is higher so the error on his first arrival times is smaller. However, the interpretation of Allen Cogbill's refraction data supports the velocity models and depth models obtained from SMU's refraction data. The weathered layer pinches out similar to the SMU depth model; however, it occurs 20 meters closer to the LANL 150 lb. shot hole.

LANL Data

Data was also obtained from the three small-scale high explosive shots conducted by the Geophysics Group, EES-3, LANL and SMU (Edwards, Pearson and Baker 1994). The three shots labeled P9, P10 and P11 were respectively placed at depths of 40, 30 and 8.5 meters in the same shot hole listed as the 150 lb. charge hole on Figures 4 and 5. The data is from the main instrument line that runs north-south in Figure 2. The main instrument line corresponds with the SMU and Cogbill refraction lines (see Figures 13).

Figure 14: SIPT2 Depth Model for Cog13c

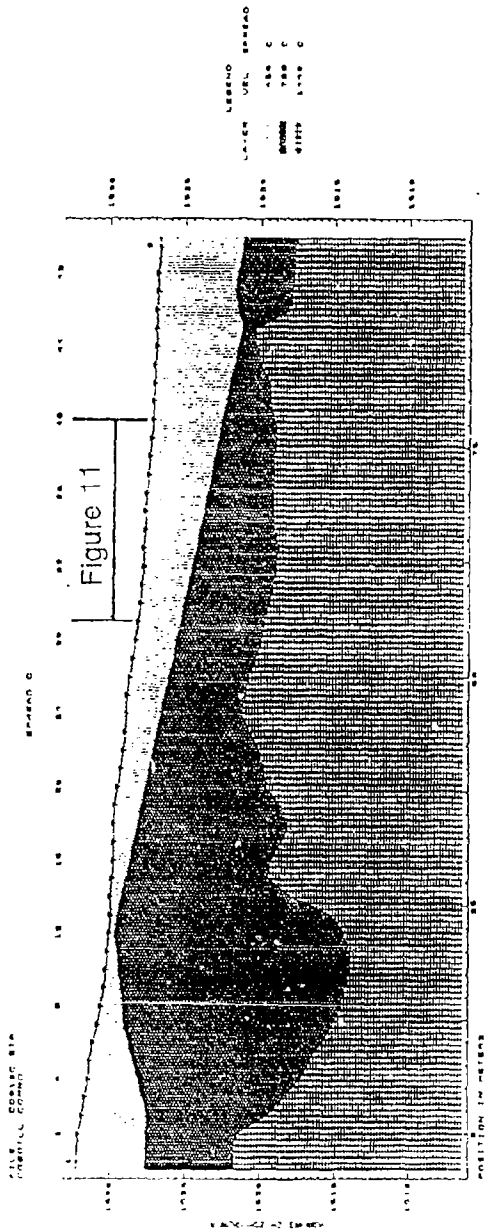

All three shots were placed at depths corresponding to layer three. Therefore, the velocities computed from the LANL shot data should be similar to the velocities obtained for layer three from SMU P wave data and Cogbill refraction data. REFRACT computed an average velocity of 1122 meters/second for layer three. The results computed by REFRACT are in Appendix S.

In SIPT2, velocity overrides of 270 m/s and 760 m/s for layers one and two respectively were entered based on earlier analysis. SIPT2 computed an average velocity of 1144 m/s for layer three. A file labeled LANLC was created that consisted of one array with three shotpoints. Like the combined files in the SMU data and Cogbill data, LANLC provides a more accurate velocity model than the three spreads (P9, P10 and P11) alone. The computed velocity for layer three from LANLC is 1143 m/s. The output files for SIPT2 are in Appendix T.

Since P11 was close to corresponding with layer two, the data was also interpreted with some of the data points assigned to layer two. The resulting output file was labeled LANL P11B. REFRACT computed the following velocities:

layer two = 641 m/s

layer three = 1150 m/s.

SIPT2 computed the following velocities:

layer two = 506 m/s

layer three = 1189 m/s.

Since velocity overrides were entered for layers one and two, there were no depth points for SIPT2 to compute depth models for the LANL data. However, the LANL velocity model supports the velocity models obtained from the SMU refraction data.

SUMMARY

The SMU refraction data, Cogbill data and LANL data support a consistent velocity model for the Grefco perlite mine. The P wave data produces the following velocity model:

layer one = 266 meters/second

layer two = 645 meters/second

layer three = 1210 meters/second.

The data also supports a consistent depth model. The first layer varies in thickness from 0.1 meters to 2.0 meters and represents the weathered zone of perlite. The second layer varies in depth from 6.5 meters to 10.0 meters from the surface. The second layer could be due to a change in the depositional flow banding or an overburden effect.

CONCLUSIONS

The SMU refraction data provided a consistent velocity and depth model for the Grefco perlite mine, and the Cogbill data and LANL data supported the velocity and depth model obtained from the SMU refraction data. Both high stress and low stress sources were used to generate energy for these experiments. With the exception of Cogbill's slightly faster P wave velocities, both types of sources yielded similar P wave velocities. The high resolution of the data set allowed a more refined depth model to be computed and helped to constrain the velocities. Finally, both interpretation programs calculated similar velocities. However, due to the complex structural nature of the site the more complex SIP program was needed to create realistic depth models.

RECOMMENDATIONS

The complex nature of the material and structure suggests that a more comprehensive refraction study (including azimuthal arrays) is needed to better understand the structural effects on the seismic waveforms. In future experiments, a preliminary refraction study should be conducted to obtain preliminary velocity and depth models needed to help design ground motion experiments. Later, a refined refraction study (based on the preliminary refraction study) should be conducted to further refine the preliminary velocity and depth models.

In all refraction studies, digital data should be obtained rather than analog. The digital data can be processed in several ways after the refraction study is finished unlike analog data. Interpretation programs like REFRACT and SIP should be used in conjunction when doing preliminary interpretations of refraction data. When interpreting refraction data from secondary refraction studies, programs capable of producing more complex depth models like SIP should be used.

Refraction studies should always use both P wave and shear wave data. Shear wave data can be harder to interpret than P wave data, but the use of digital data would help to identify first arrivals. Velocity models and depth models should be computed using both P wave and shear wave data, and the models should be consistent with each other.

The model may later be refined by generating synthetic seismograms for the model and comparing them to the actual data. Further refinement of the model can be done by using surface wave dispersion to determine the shear wave velocity and structure (Craven 1992).

REFERENCES

Craven, Mike E. 1992. Shear Wave Velocity Determination Using Surface Wave Dispersion. M.S. Thesis. Southern Methodist University.

Edwards, C. L., D. Craig Pearson, and Diane F. Baker. 1994. Ground Motion Data from the Small-Scale Explosive Experiments Conducted at the Grefco Perlite Mine Near Socorro, New Mexico.

Pakiser, L. C., and R. A. Black. 1957. "Exploring for Ancient Channels With the Reafraction Seismograph." Geophysics 22.1: 32-47.

Redpath, Bruce B. 1973. Seismic Refraction Exploration for Engineering Site Investigations.

Rimrock Geophysics. 1-93. SIP Shell. Computer software.

Rimrock Geophysics. 1994. SIPIN and SIPEDT. Version 4.1. Computer software.

Rimrock Geophysics. 1994. SIPT2. Version 4.1. Computer software.

Scott, James H. 1973. "Seismic Refraction Modeling by Computer." Geophysics 38.2: 271-284.

Scott, James H., Richard G. Burdick, and Harry Ludowise. 1988. "Interpretation of Seismic Refraction Data on a Microcomputer." Proceedings of the Annual Highway Geology Symposium 39: 402-421.

Scott, James H. and Richard D. Markiewicz. 1990. "Dips and Chips -- PC Programs for Analyzing Seismic Refraction Data." Proceedings, SAGEEP 1990, Golden, Colorado, pp. 175-200

Sjogren, B. et al. 1984. Shallow Refraction Seismics. New York: Chapman & Hall.